Int. J. Electrochem. Sci., 7 **(2012)** 5962 - 5976

International Journal of
ELECTROCHEMICAL
SCIENCE
www.electrochemsci.org

A Novel Electrospinning Application for Polyvinyl Chloride Nanofiber Coating Deposition as a Corrosion Inhibitor for Aluminum, Steel, and Brass in Chloride Solutions

Mahir Es-saheb[1], *Ahmed A. Elzatahry*[2,3*], *El-Sayed M. Sherif*[4,5], *Ahmad S. Alkaraki*[1], *El-Refaie kenawy*[6]

[1] Mechanical Engineering Department, King Saud University, P.D. Box 800, Riyadh 11421, Saudi Arabia
[2] Petrochemical Research Chair, Chemistry Department, College of Science, King Saud University, B.O. Box 2455 Riyadh 11451, Saudi Arabia
[3]Advanced Technology and New Materials Research Institute, City of Scientific Research and Technology Applications, New Boarg El-Arab City, Alexandria, Egypt.
[4] Center of Excellence for Research in Engineering Materials (CEREM), Advanced Manufacturing Institute, King Saud University, P. O. Box 800, Riyadh 11421, Saudi Arabia.
[5] Electrochemistry and Corrosion Laboratory, Department of Physical Chemistry, National Research Centre (NRC), Dokki, 12622 Cairo, Egypt.
[6] Chemistry Department, Polymer Research Group, Faculty of Science, Tanta University, Tanta 31527, Egypt.
[*]E-mail: aelzatahry@ksu.edu.sa

Received: 13 May 2012 / *Accepted:* 9 June 2012 / *Published:* 1 July 2012

Electrospinning is a unique technology that can produce nano-woven fibrous structures with fiber diameters ranging from tens of nanometers to microns. In this work the novel application of this technique as a coating process was investigated and presented. Thus, the electrospun polymer nanofiber coating of PVC was successfully deposited on aluminum, steel and brass. The coated samples were then tested to assess the corrosion properties and the characteristics of the coated surfaces in 3.5 wt.% NaCl solutions using cyclic potentiodynamic polarization (CPP) and electrochemical impedance spectroscopy (EIS). The morphologies and the microstructures of the nanofiber coatings are characterized and assessed using scanning electron microscopy (SEM) and thermal degradation analysis (TGA). The nanofiber coatings were of diameters from 80 to 100 nm and lengths from 3 to 5 µm and were compact and entangled with each other. This new promising success of the electrospinning process for coating is believed to have a big impact on corrosion and maintenance cost savings in the various industries.

Keywords: Electrospinning; Metals and alloys corrosion; Nanofiber coatings; PVC; Corrosion Inhibitor

1. INTRODUCTION

Electrospinning is a unique technology that can produce nano-woven fibrous structures with fiber diameters ranging from tens of nanometers to microns. It has been widely used in various applications in many fields such like, medical, Energy, engineering, and nano-industry [1-3]. In the last few years electrospinning process attracted increasing attention from the research community. Recently, a huge number of research works, on the process parameters, materials, characterization, and applications has been published [1-5].

When the diameters of polymer fiber materials are shrunk from micrometers to submicrons or nanometers, there appear several amazing characteristics such as large surface area to volume ratio, flexibility in surface functionalities, and superior mechanical performance (e.g. stiffness and tensile strength) compared with any other known form of the material. These outstanding properties make the polymer nanofibers to be optimal candidates for many important applications. A number of processing techniques such as drawing [6], template synthesis [7], phase separation [8], self-assembly [9], and electrospinning [10] have been used to prepare polymer nanofibers in recent years.

There are many ways to design nanostructured coatings, such as in the form of nanocomposite coatings, nano-scale multilayer coating, super-lattice coating, and nano-graded coatings. Designing of nanostructured coatings will depend on the applications and needs consideration of many factors such as the interface volume, crystallite size, single layer thickness, surface and interfacial energy, texture, epitaxial stress and strain, etc., all of which depend on materials selection, deposition methods and process parameters [11]. Good mechanical properties of a coating require high hardness, high toughness, low friction, high adhesion strength on a substrate, good load support capability, chemical and thermal stability. However, inspire these intensive investigations carried out on the various processes and their parameters and applications and reported in the literature, little or no work has been reported on coating aspects using electrospinning technique.

Coatings impart specific engineering properties of a substrate material by modifying or applying a thin layer at its surface. A nanocoating is a coating that comprises of at least one constituent with dimensions in nano-scale. Small particle size (nanoscale) imparts nanocoatings with a large number of surface atoms, high surface energy, spatial confinement and reduced imperfections resulting in improved physical, mechanical, chemical and optoelectronic properties. Due to this reason, there is considerable interest among researchers to use nanomaterials for a range of products including nanocoatings [12, 13] with improved strength, hardness, corrosion behavior and/or increased wear-, friction-, abrasion- and scratch resistance. The availability of nanoparticles has spurred the development of nanocoatings with superior properties. Nanocoatings find wide ranging utilization in optical, magnetic, electronic, catalytic, mechanical, chemical and tribological applications. They are used in high speed machining [14], tooling [15], optical equipment [16], magnetic storage devices [17] and bearings, engine parts and seals [18].

There is an increasing demand placed by legislation to use coatings which are environmentally friendly and thereby minimize damage to the environment. For instance, there is a need to replace chromate conversion coatings widely used to protect Al alloys against corrosion due to their deleterious effect on human health. Many alternative coatings based on manganese [19], molybdenum

[20], vanadium [21], cerium [22] and silica [23] have been used. Silica based coatings have been suggested as one of the most environmentally friendly alternatives to chromate conversion coatings for the protection of Al alloys. However, no or little researches are found on coatings using electro-spinning technique. Careful control of parameters such as composition, voltage, injection pressure and speed, temperature and over potential is required to produce optimal electrospun fibers.

For the present study, the novel use of a polymeric material will be explored to prepare corrosion resistant coatings using electrospinning deposition of nanofiber of polyvinyl chloride (PVC) on aluminum, stainless steel and brass substrates. The corrosion tests were obtained by using cyclic potentiodynamic polarization and electrochemical impedance spectroscopy measurements. The surfaces of Al, brass and their PVC coated surfaces before and after performing the corrosion techniques were investigated using scanning electron microscope and energy dispersive X-ray analyzer.

2. MATERIALS AND EXPERIMENTAL TECHNIQUES

2.1 Electrospinning setup

The polymer solutions were electrospun using a needleless laboratory machine called a nano spider laboratory (NSLAB 500S), which consists of a spinning head tube where the rotating spinning electrode is wetted in solution under high voltage. Nanofibers are coating exchangeable substrate belt which is moving along the static collecting electrode. Internal control parameters of the process are electrode distance, high voltage, electrode speed and substrate speed. External parameters used for control of electrospinning throughput and nanofiber quality are solution characteristics (viscosity, conductivity) and air properties (temperature, relative humidity).

2.2 Electrospinning of PVC

Processing of polymer nanofiber was generally as follows; The PVC solution in a concentration of 12 wt.% was prepared by dissolving the polymer pellets in a tetrahydrofuran (THF) solvent at 30^{o}C and stirring overnight to be used for electrospinning the nanofiber on Steel, aluminum and brass surfaces.

The polymer solution was spun under the following conditions; distance from the active electrode to collecting electrode is 18 cm at a driving voltage of 70 KV, electrode speed 1.6 rounds per minute (rpm), temperature of 25^{o}C and humidity of 33%. The fibers were collected on target metals. The electrospun fibers were first air dried in the hood at room temperature (overnight quickly rinsed with distilled water; air dried again and then dried in vacuum oven overnight).

2.3 Nanofibers morphological characterization

The surface morphology of electrospun nanofibers on aluminum, stainless steel and brass surfaces were examined by scanning electron microscopy (JSM-7100F). After sputter coating with

Gold, the fiber size distribution was measured up to five frames of randomly selected SEM micrograph using software.

2.4 ThermoGravimetric Analysis

Thermo gravimetric analysis was carried out using a TA Instruments, Q500 TGA, using platinum cell in nitrogen atmosphere 20 ml/min.

2.5 Corrosion tests

The test solution, 3.5 wt.% NaCl, was prepared by dissolving 35 g of NaCl in 1 L glass flask. The aluminum, steel, and brass with and without the PVC coatings for corrosion measurements were prepared by attaching an insulated copper wire to one face of the sample using an aluminum conducting tape, and then isolated by cold mounted in resin before letting it to dry in air for 24 h at room temperature. To prevent the possibility of crevice corrosion during measurement, the interface between sample and resin was coated with Bostik Quickset, a polyacrylate resin. The area of the other face of the samples, on which the measurements were carried out, was 1.0 cm^2.

Electrochemical experiments were performed by using a PARC Parstat-2273 Advanced Electrochemical System after immersing the bare and coated PVC electrodes for 20 minutes in freely aerated stagnant 3.5 wt.% NaCl solutions. The cyclic potentiodynamic polarization (CPP) curves for aluminum were obtained by sweeping the potential from -1800 mV in the positive direction up to -500 mV vs. Ag/AgCl at a scan rate of 1 mV/s. The CPP curves for steel and brass were scanned from -1200 mV in the less positive direction up to 500 mV vs. Ag/AgCl at the same scan rate for aluminum. For electrochemical impedance spectroscopy (EIS) experiments, the frequency was scanned at the open-circuit potential from 100 kHz to 0.1 Hz with an ac wave of ±5 mV peak-to-peak overlaid on a dc bias potential, and the Nyquist plots were acquired using Powersine software at a rate of 10 points per decade change in frequency.

3. RESULTS AND DISCUSSION

3.1. Optical microscopy (OM) investigations

The OM micrographs for (a) bare aluminum, (b) PVC coated aluminum, (c) bare steel, (d) PVC coated steel, (e) bare brass, and (f) PVC coated brass, respectively are shown in Fig. 1. It is clearly seen from Fig. 1 that, the PVC coated images show that the PVC layers on the surface are compact and look homogeneously distributed on the surface. The coating of aluminum, steel and brass with PVC led also to changing the morphology and color of their surfaces.

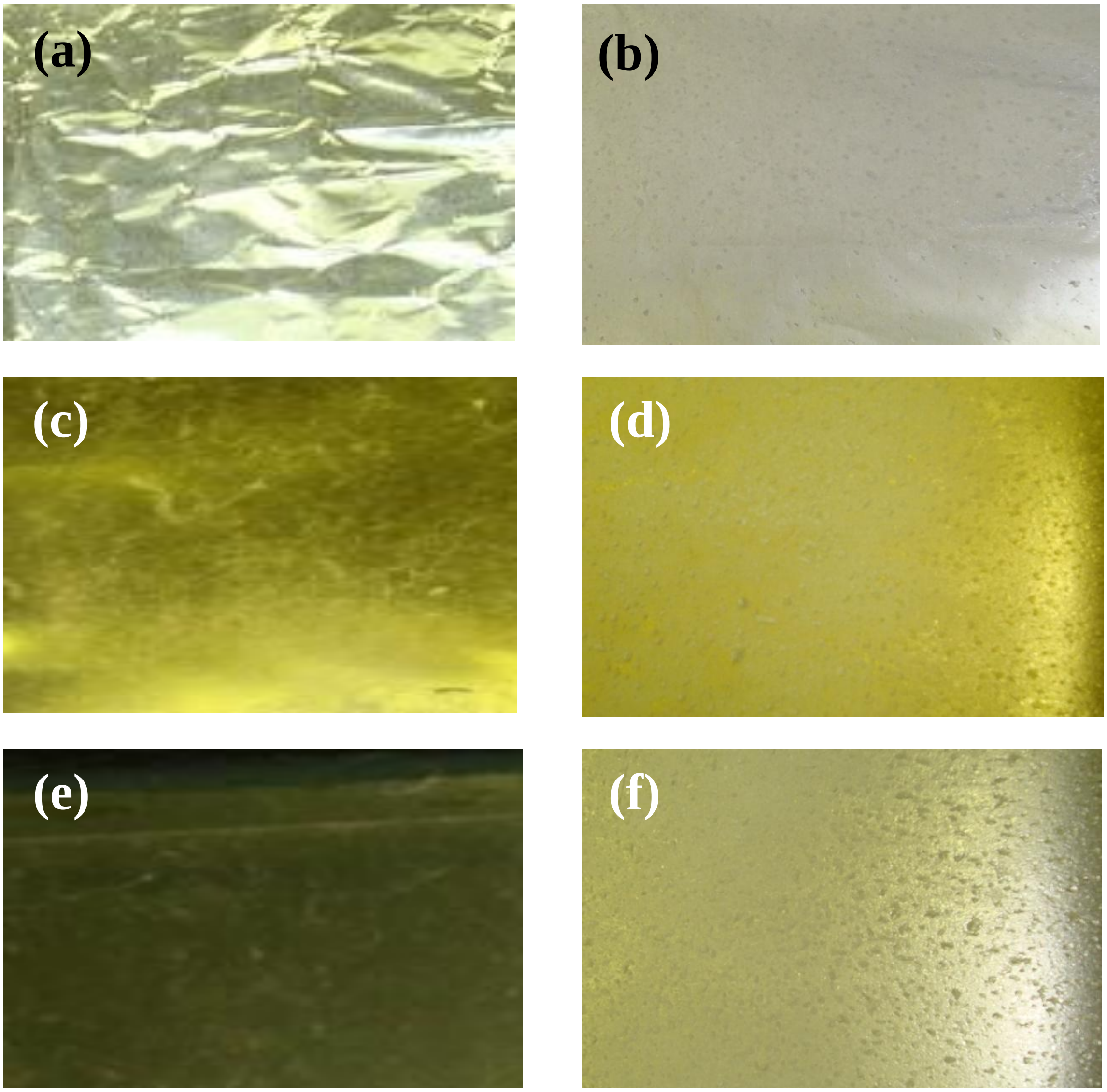

Figure 1. The optical microscopy images for aluminum, stainless steel, and brass surfaces before and after PVC coating using the electrospinning technique.

3.2. Thermal degradation analysis

The thermal behavior of prepared PVC electrospun fiber was characterized by thermal degradation analysis (TGA). The TGA thermogram in nitrogen atmosphere for electrospun PVC fiber is shown in Fig.2. The results revealed that PVC electrospun fiber decomposes in three stages. The weight loss at 29.51 - 170 °C was due to the loss of humidity water and the water of crystallinity. The weight loss at the stage 220 - 336.80 °C was due to dechloronation and the formation of intermediate. On the other hand, the weight loss at the last stage 400.00 - 450.50 °C was probably due to decomposition to carbon oxide and volatile hydrocarbons [24].

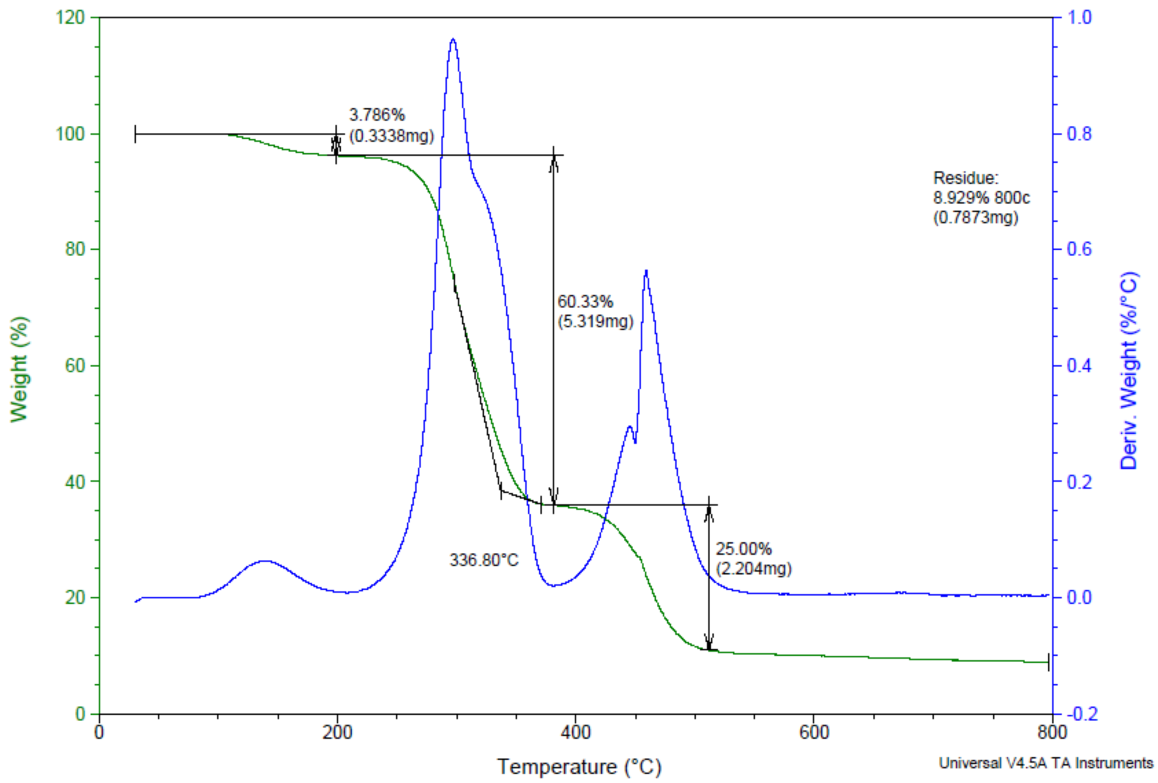

Figure 2. The TGA thermogram in nitrogen atmosphere for electrospun PVC fiber.

3.3. Cyclic potentiodynamic polarization (CPP) measurements

In order to report the corrosion parameters for uncoated and coated aluminum, steel, and brass in the freely aerated stagnant 3.5 wt.% NaCl solution, CPP experiments were carried out. Fig. 3 shows the CPP curves obtained for (a) bare Al and (b) Al coated with PVC electrodes after their immersion for 20 min in freely aerated 3.5 wt.% NaCl solutions. Similar CPP curves were also obtained for bare and coated steel and brass in 3.5 wt.% NaCl solutions as shown in Fig. 4 and Fig. 5, respectively. The corrosion parameters, cathodic (β_C) and anodic (β_a) Tafel slopes, corrosion potential (E_{Corr}), corrosion current (j_{Corr}), pitting potential (E_{Pit}), protection potential (E_{Prot}), polarization resistance (R_P), and corrosion rate (K_{Corr}), obtained from the polarization curves shown in Fig. 3, Fig. 4 and Fig. 5 are presented in Table 1. Some of these parameters were calculated as previously reported in our work [25-35]. The values of R_P and K_{Corr} were calculated from the polarization data as follows [36-45]:

$$R_P = \frac{1}{j_{Corr}}\left(\frac{\beta_c . \beta_a}{2.3(\beta_c + \beta_a)}\right) \tag{1}$$

$$K_{Corr} = \frac{j_{Corr}\, k\, E_W}{d\, A} \tag{2}$$

Where, k is a constant that defines the units for the corrosion rate (= 3272 mm/ (amp. cm. year)), E_W the equivalent weight in grams/equivalent of the tested materials (E_W = 9 for Al, = 27.9 for steel, and = 32.1 grams/equivalent for brass), d the density in g cm^{-3} (d = 2.7 for Al, = 7.85 for steel, and = 8.32 g/cm^3), and at the area of the exposed surface of the electrode in cm^2 (A = 1 cm^2 for all materials).

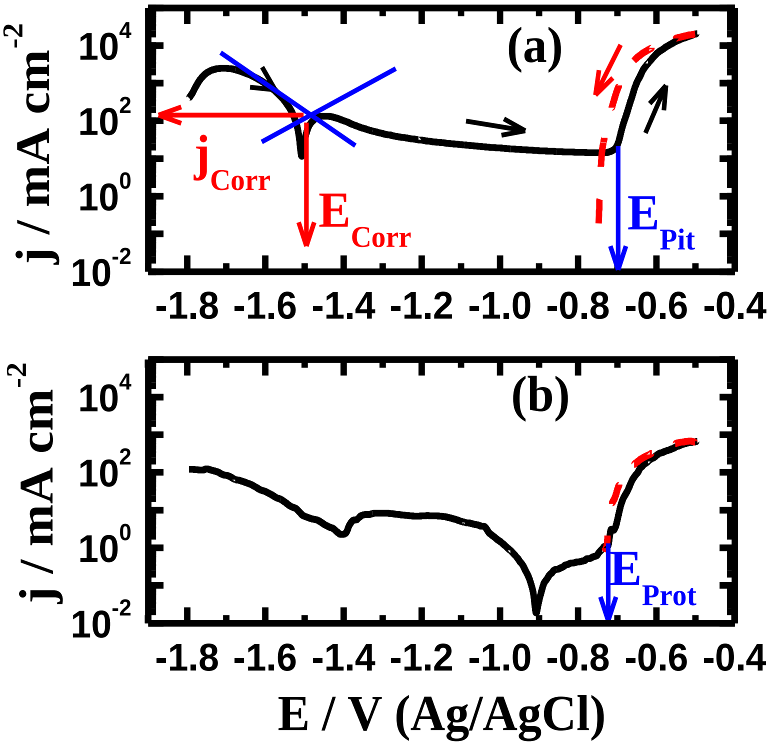

Figure 3. Cyclic potentiodynamic polarization curves obtained for (a) bare Al, (b) and (b) Al coated with PVC electrodes after their immersion for 20 min in freely aerated 3.5 wt.% NaCl solutions.

It is clearly seen from the polarization curves shown in Fig. 3, Fig. 4, Fig. 5 and Table 1 that the PVC coated samples show lower cathodic and anodic currents and lower values of j_{Corr}, anodic currents and K_{Corr}. This effect also largely shifted the E_{Corr} to the less negative potential values as well as highly increased the values of R_P. The presence of PVC coatings on the surfaces of the tested materials prevented to a great extent their dissolution in the chloride solution. For example, aluminum is well known to develop an oxide film on its surface when exposed to near neutral aerated solutions on two steps according to the following reactions [46-53],

$$\mathrm{Al_{(S.)ads.}} + 3\mathrm{OH^-} = \mathrm{Al(OH)_{3,ads.}} + 3e^- \quad (3)$$

$$2\mathrm{Al(OH)_{3,ads.}} = \mathrm{Al_2O_3{\cdot}3H_2O} \quad (4)$$

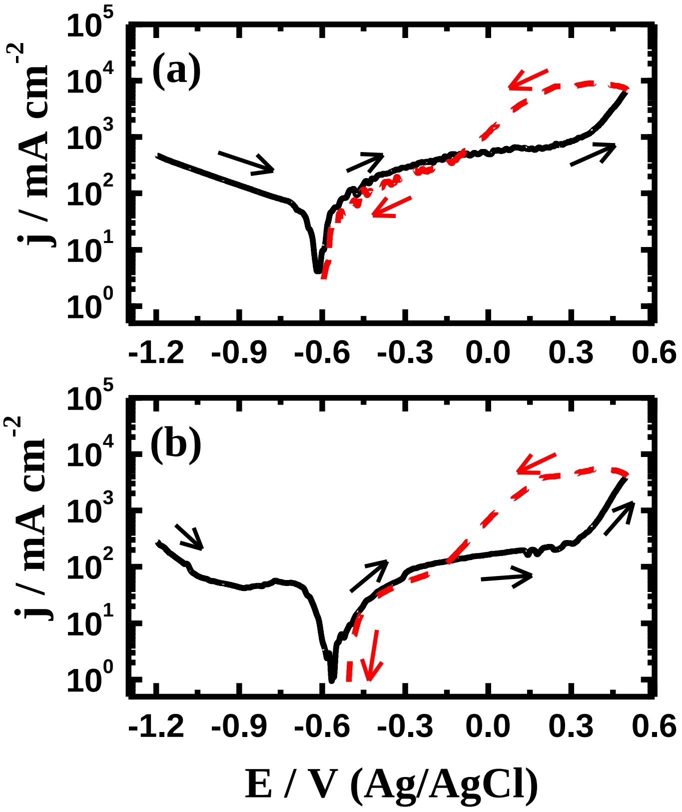

Figure 4. Cyclic potentiodynamic polarization curves obtained for (a) bare stainless steel and (b) stainless steel coated with PVC electrodes after their immersion for 20 min in freely aerated 3.5 wt.% NaCl solutions.

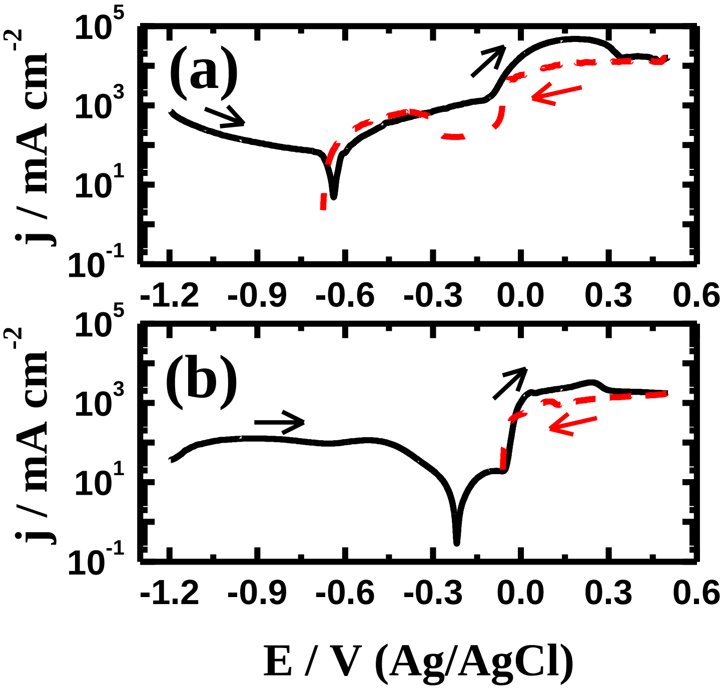

Figure 5. Cyclic potentiodynamic polarization curves obtained for (a) bare brass and (b) brass coated with PVC electrodes after their immersion for 20 min in freely aerated 3.5 wt.% NaCl solutions.

In the presence of high concentrations of chloride ions, 3.5 wt.% NaCl solutions, pitting corrosion occurs due to the breakdown of the formed oxide film [46,47]. At these conditions, the chloride ions attack the weak parts of the oxide film and reach the aluminum surface to produce aluminum chloride complex as follows,

$$Al^{3+} + 4Cl^{-} = AlCl_4^{-} \qquad (5)$$

The Al(III) resulted due to the chloride ions attack and the application of the negative potential (Fig. 3a) on the aluminum surface as previously reported [46],

$$Al = Al^{3+} + 3e^{-} \qquad (6)$$

The formation of $AlCl_4^{-}$ complex compound (Eq. 5) leads to the occurrence of pitting corrosion due to its diffusion into the bulk of the solution [46-50]. The chloride ions may work by adsorption onto the aluminum surface and then react with Al(III) that is existed in the aluminum oxide lattice and form an oxychloride complex, $Al(OH)_2Cl_2^{-}$, as stated by Eq. (7). This complex dissolves into the solution once it is formed, which leads to increasing the corrosion rate of Al.

$$Al^{3+}_{\text{(in crystal lattice of the oxide)}} + 2Cl^{-} + 2OH^{-} = Al(OH)_2Cl_2^{-} \qquad (7)$$

On the other hand and according to the data listed in Table 1, the coated Al surface showed much less corrosion current and corrosion rate and high polarization resistance because the dissolution reactions seen by Eqs 5-7. This indicates that the PVC coating provides high corrosion protection to the aluminum surface. This effect is also provided for the PVC coated steel and brass surfaces as shown by Table 1, Fig. 4 and Fig. 5.

Table 1. Parameters obtained from polarization curves shown in Fig. 3, Fig. 4 and Fig. 5 for aluminum, steel, and brass electrodes, respectively after their immersion in 3.5% NaCl solutions for 20 min before measurement.

Material	Parameter							
	$-\beta c$ / V dec^{-1}	E_{Corr} / V	j_{Corr} / μA cm^{-2}	βa / V dec^{-1}	E_{Pit} / V	E_{Prot} / V	Rp / kΩ cm^{2}	K_{Corr} / mmy^{-1}
Bare Al	0.11	–1.485	100	0.11	–0.70	-0.745	0.24	1.091
Al coated PVC	0.12	–0.890	0.25	0.21	–0.710	-0.730	132.8	0.0027
Steel	0.36	–0.630	60	0.30	0.300	-0.105	1.17	0.698
Steel coated PVC	0.21	–0.540	13	0.275	0.345	-0.150	3.98	0.151
Brass	0.30	–0.670	78	0.21	–	–	0.69	0.985
Brass coated PVC	0.15	–0.225	8.5	0.21	–	–	4.46	0.107

3.3. Electrochemical impedance spectroscopy (EIS) measurements

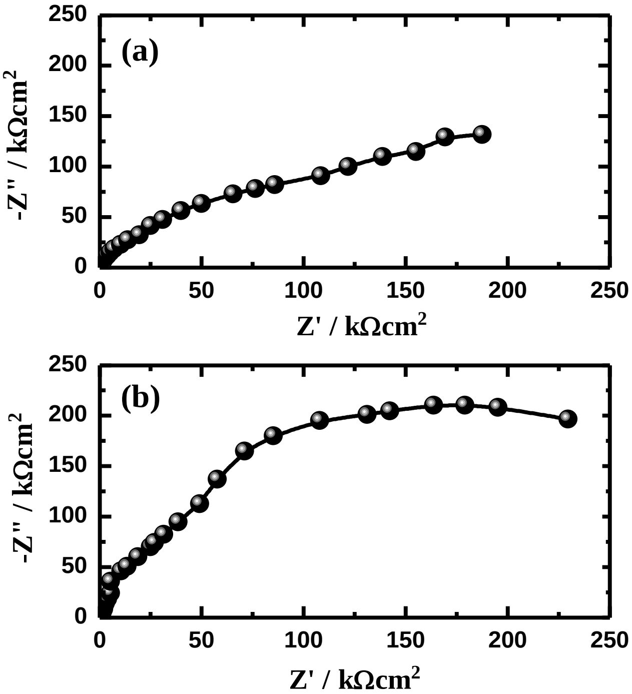

Figure 6. EIS Nyquist plots obtained for (a) bare Al and (b) Al coated with PVC electrodes after their immersion for 20 min in freely aerated 3.5 wt.% NaCl solutions.

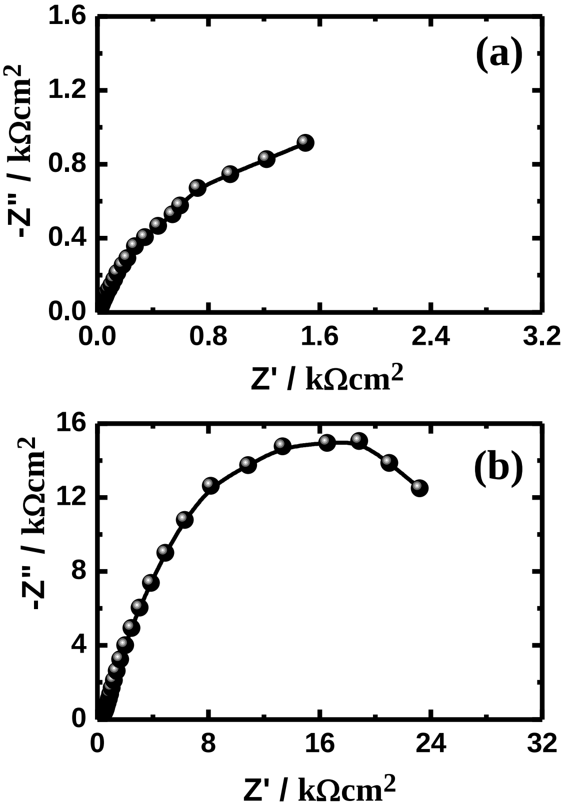

Figure 7. EIS Nyquist plots obtained for (a) bare stainless steel and (b) stainless steel coated with PVC electrodes after their immersion for 20 min in freely aerated 3.5 wt.% NaCl solutions.

EIS technique provides important mechanistic and kinetic information for an electrochemical system under investigation [46,47,54-59]. The method was successfully employed to explain the pitting and passivation phenomena on Al [46-50], copper [54-59] and iron [27,45,60] in chloride solutions. Typical Nyquist impedance plots obtained for (a) bare Al and (b) PVC coated Al electrodes at an open-circuit potential after 20 min immersion in 3.5 wt.% NaCl solutions are shown in Fig. 6. The EIS spectra were also obtained at the same conditions on (a) bare and (b) PVC coated electrodes of steel and brass as respectively shown in Fig. 7 and Fig. 8.

It is clearly seen from Fig. 6 that the Al electrode shows only a single but distorted semicircle is observed for the Al electrode regardless of whether the surface is coated or not. Coating the Al surface with PVC increased the diameter of the semicircle indicating that the surface is more passivated. Here, the semicircles at high frequencies are generally associated with the relaxation of electrical double layer capacitors and the diameters of the high frequency semicircles can be considered as the charge transfer resistance [61]. This effect at high frequencies is due to the decrease of the electrochemical active and flawed areas on the aluminum surface by both stabilizing the formed oxide film on Al, which increases in case of PVC coated surface. As well as, the diameter of the semicircle for Al at low frequency also increased for the coated PVC sample. This is due to the increase of the aluminum impedance values, which in turn indicates on the high passivation of the surface against corrosion [53].

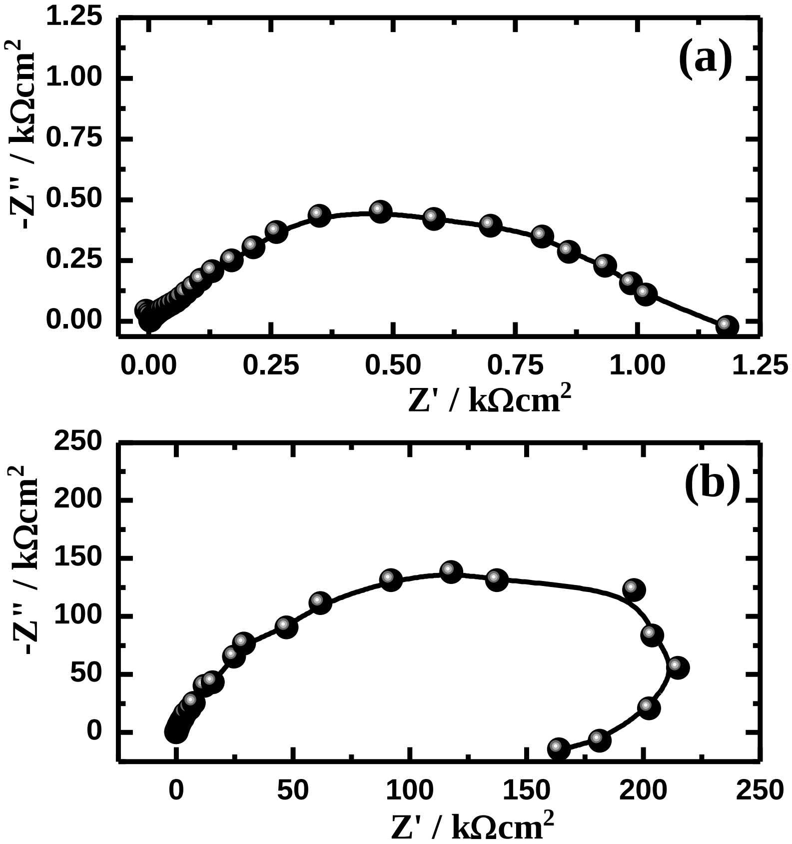

Figure 8. EIS Nyquist plots obtained for (a) bare brass and (b) brass coated with PVC electrodes after their immersion for 20 min in freely aerated 3.5 wt.% NaCl solutions.

The EIS Nyquist plots for steel and brass (Fig. 7 and Fig. 8, respectively) showed much better behavior compared to that obtained for Al, Fig. 6. Where, the diameter of the semicircle was increasing in case of steel by about 10 times more and for brass recorded about 200 times bigger. This confirms the data obtained by polarization curves shown in Fig. 3, Fig. 4 and Fig. 5 that coating Al, steel and brass with PVC nanofiber passivates their surface to the extent that precludes their corrosion reactions in the 3.5 wt.% test solution.

3.4. Scanning electron microscopy (SEM) investigations

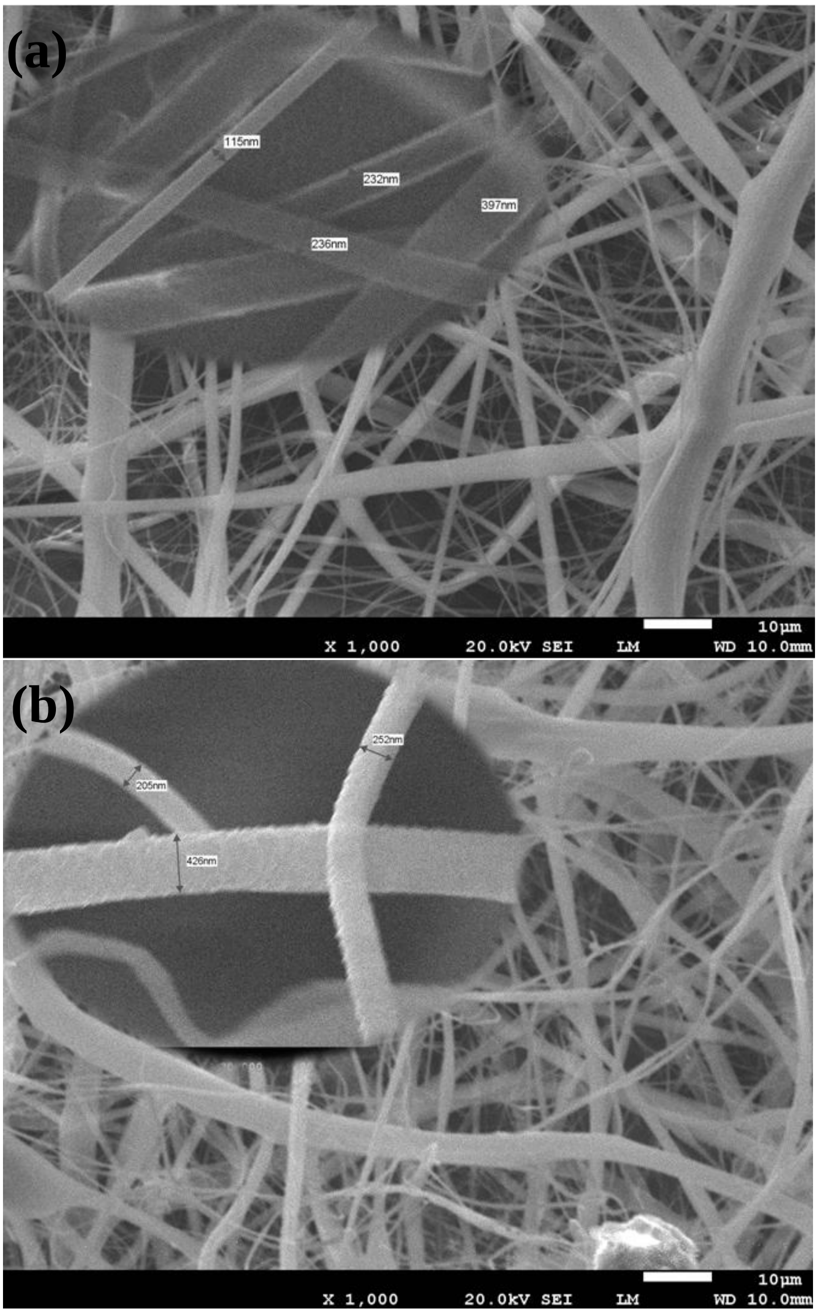

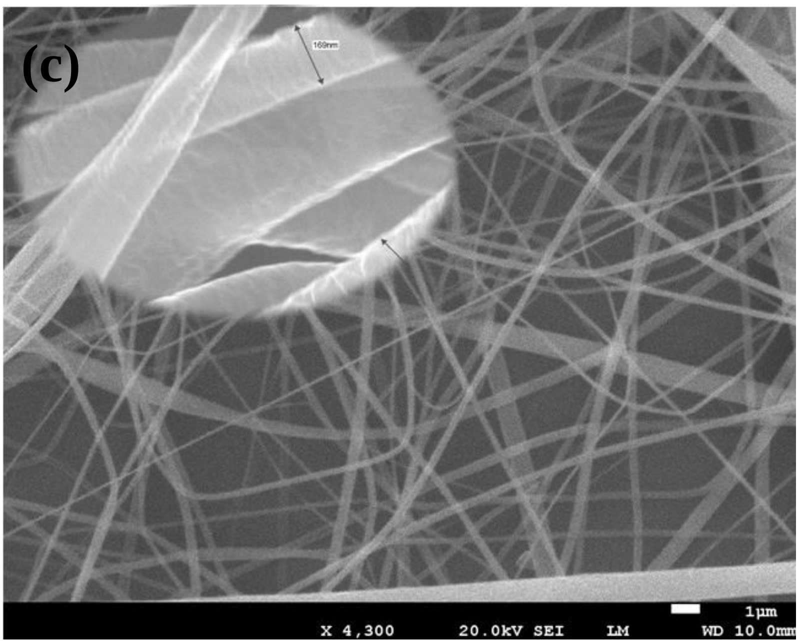

Figure 9. SEM images for PVC electrospun fiber coated over (a) aluminum, (b) steel, and (c) brass plates.

The morphology, structure and the distribution of the PVC on the coated surfaces were also investigated using SEM. Fig. 9 shows the SEM micrographs for the PVC coated surfaces on (a) aluminum, (b) steel, and (c) brass, respectively. It is clearly seen that the SEM images exhibit a web of random oriented fiber with abroad distribution from 115 to 400 nm in case of PVC/Al sample, from 160 to 400 nm in case of PVC/steel sample, and from 200 to 400 nm in case of PVC/brass sample.

4. CONCLUSION

In this investigation, we have successfully fabricated an electrospun polymer nanofiber coating of PVC on aluminum, steel and brass surfaces. The surface morphology of these materials with and without coatings was examined using optical microscope. The effect of PVC coatings on the corrosion behavior of aluminum, steel, and brass in 3.5 wt.% NaCl solutions was also tested using both cyclic potentiodynamic polarization (CPP) and electrochemical impedance spectroscopy (EIS) measurements. The morphologies and the microstructures of the nanofiber coatings are characterized and assessed using scanning electron microscopy (SEM) and thermal degradation analysis (TGA). CPP measurements indicated that the materials coated with PVC showed much lower corrosion currents and corrosion rates and higher polarization resistances compared to the uncoated samples. The PVC coating also shifted to the corrosion potential towards the less negative potential for all materials. EIS spectra confirmed that the PVC coated surfaces provided semicircles with larger diameters, which indicates that these surfaces are more passivated. All measurements were in good agreement and confirmed that the deposited PVC coatings can to a great extent protect the aluminum, steel, and brass surface against corrosion in 3.5 wt.% NaCl solution.

ACKNOWLEDGEMENTS
The authors extend their appreciation to the Deanship of Scientific Research at King Saud University for funding the work through the research group project No RGP-VPP-036.

References

1. Zheng-Ming Huanga, Y.-Z. Zhangb, M. Kotakic, S. Ramakrishnab, *Compos. Sci. Technol*., 63 (2003) 2223.
2. Derrell H. Renker, Haoqing Hou, Electrospinning. Encyclopedia of Biomaterials Biomedical Engineering, 31 August (2004).
3. D. Luck, A. Sarkar, L. Martinov, K. Vodsed Ikov, D. Lubasov, J Chaloupec, P. Pokorn, P. Mike, J.Chvojka, M. Komrek, Journal Textile Progress, 41(2009) 559.
4. Feng-Lei Zhou, Rong-hua Gong, Isaac Porat, *Polymer International*, 58 (2009) 331.
5. J.M. Deitzel, J. Kleinmeyer, J.K. Hirvonen, T.N.C. Beck, *Polymer*, 42 (2001) 8163.
6. T. Ondarcuhu, C. Joachim, *Europhys. Lett.*, 42 (1998) 215.
7. L. Feng, S. Li, H. Li, J. Zhai, Y. Song, L. Jiang, et al., *Angew Chem. Int.* Ed., 41 (2002) 1221.
8. P.X. Ma, R. Zhang, *J. Biomed. Mat. Res*., 46 (1999) 60.
9. G.M. Whitesides, B. Grzybowski, *Science,* 295 (2002) 2418.
10. H. Fong, D.H. Reneker In: D.R. Salem, Editor, *Structure formation in polymeric fibers,* Munich, Hanser, (2001) p. 225–46.
11. Th. Lampke, A. Leopold, D. Dietrich, G. Alisch, B. Wielage, *Surf. Coat. Technol.*, 201 (2006) 3510.
12. F. Vaz, L. Rebouta, *Mater. Sci. Forum*, 383 (2002) 143.
13. R.A. Andrievski, *Mater. Trans. 42,* (2001) 1471.
14. S. Veprek, A.S. Argon, *Surf. Coat. Technol.*, 146–147 (2001) 175.
15. V. Provenzano, R.L. Holtz, *Mater. Sci. Eng. A*, 204 (1995) 125.
16. L. Maya, W.R. Allen, *J. Vac. Sci. Technol.*, B 13 (2) (1995) 361.
17. R.A. Andrievski, A.M. Gleze, *Scripta Mater.*, 44 (2001) 1621.
18. S.C. Tjong, Haydn Chen, *Materials Science and Engineering R*, 45 (2004) 1-88.
19. L.S. Kasten, J.T. Grant, N. Grebasch, N. Voevodin, F.E. Arnold, M.S. Donley, *Surf. Coat. Technol.*, 140 (2001) 11.
20. A.S. Hamdy, A.M. Beccaria, *J. Appl. Electrochem.*, 35 (2005) 467.
21. R.L. Cook Jr., S.R. Taylor, *Corrosion*, 56 (2000) 321.
22. A.S. Hamdy, A.M. Beccaria, P. Traverso, *J. Appl. Electrochem.*, 35 (2005) 473.
23. K. Aramaki, *Corros. Sci.*, 43 (2001) 591.
24. Bo Wu, Shuhua Qi, Xin Wang, *Polymer Testing*, 29 (2010) 717.
25. El-Sayed M. Sherif, R.M. Erasmus, J.D .Comins, *J. Appl. Electrochem.*, 39 (2009) 83.
26. El-Sayed M. Sherif, R.M. Erasmus, J.D. *Comins, Corros. Sci.*, 50 (2008) 3439.
27. El-Sayed M. Sherif, *Mater. Chem. Phys*., 129 (2011) 961.
28. El-Sayed M. Sherif, R.M. Erasmus, J.D. Comins, *J. Colloid Interface Sci*., 309 (2007) 470.
29. J.H. Potgieter, P.A. Olubambi, L. Cornish, C.N. Machio, El-Sayed M. Sherif, *Corros. Sci.*, 50 (2008) 2572.
30. El-Sayed M. Sherif, J.H. Potgieter, J.D. Comins, L. Cornish, P.A. Olubambi, C.N. Machio, *Corros. Sci*., 51 (2009) 1364.
31. El-Sayed M. Sherif, *J. Solid State Electrochem.*, 16 (2012) 891.

32. El-Sayed M. Sherif, *Int. J. Electrochem. Sci.*, 7 (2012) 1884.
33. El-Sayed M. Sherif, *Int. J. Electrochem. Sci.*, 7 (2012) 2374.
34. El-Sayed M. Sherif, J. H. Potgieter, J. D. Comins, L. Cornish, P. A. Olubambi, C. N. Machio, J. Appl. Electrochem. 39 (2009) 1385.
35. E.M. Sherif, S.-M. Park, Electrochim. Acta 51 (2006) 4665.
36. Khalil A. Khalil, El-Sayed M. Sherif, A.A. Almajid, *Int. J. Electrochem. Sci.*, 6 (2011) 6184.
37. El-Sayed M. Sherif, *Int. J. Electrochem. Sci.*, 6 (2011) 2284.
38. El-Sayed M. Sherif, A.A. Almajid, A.K. Bairamov, Eissa Al-Zahrani, *Int. J. Electrochem. Sci.,* 6 (2011) 5430.
39. El-Sayed M. Sherif, A.A. Almajid, A.K. Bairamov, Eissa Al-Zahrani, *Int. J. Electrochem. Sci.,* 7 (2012) 2796.
40. E.M. Sherif, S.-M. Park, *Electrochim. Acta,* 51 (2006) 6556.
41. E.M. Sherif, S.-M. Park, *J. Electrochem. Soc.*, 152 (2005) B205.
42. El-Sayed M. Sherif, *Int. J. Electrochem. Sci.*, 7 (2012) 2832.
43. E. M. Sherif, S.-M. Park, *Corros. Sci.,* 48 (2006) 4065.
44. El-Sayed M. Sherif, A.A. Almajid, *J. Appl. Electrochem.*, 40 (2010) 1555.
45. El-Sayed M. Sherif, R.M. Erasmus, J.D. Comins, *Electrochim. Acta,* 55 (2010) 3657.
46. E.M. Sherif, S.-M. Park, *J. Electrochem. Soc.*, 152 (2005) B428.
47. E.M. Sherif, S.-M. Park, *Electrochim. Acta,* 51 (2006) 1313.
48. El-Sayed M. Sherif, *Int. J. Electrochem. Sci.* 6 (2011) 1479.
49. F.H. Latief, El-Sayed M. Sherif, A.A. Almajid, H. Junaedi, *J. Anal. Appl. Pyrolysis,* 92 (2011) 485.
50. El-Sayed M. Sherif, A.A. Almajid, F.H. Latif, H. Junaedi, *Int. J. Electrochem. Sci.,* 6 (2011) 1085
51. El-Sayed M. Sherif, E.A. El-Danaf, M.S. Soliman, A.A. Almajid, *Int. J. Electrochem. Sci.,* 7 (2012) 2846.
52. El-Sayed M. Sherif, F.H. Latif, H. Junaedi, A.A. Almajid, *Int. J. Electrochem. Sci.,* 7 (2012) 4352.
53. El-Sayed M. Sherif, Effects of 3-Amino-1,2,4-triazole-5-thiol on the Inhibition of Pure Aluminum Corrosion in Aerated Stagnant 3.5 wt.% NaCl Solution as a Corrosion Inhibitor, *Int. J. Electrochem. Sci.*, 7 (2012) In Press.
54. El-Sayed M. Sherif, *J. Mater. Eng. Performance,* 19 (2010) 873.
55. El-Sayed M. Sherif, A.H. Ahmed, *Synthesis and Reactivity in Inorganic, Metal-Organic, and Nano-Metal Chemistry*, 40 (2010) 365.
56. El-Sayed M. Sherif, *Int. J. Electrochem. Sci.*, 6 (2011) 3077.
57. El-Sayed M. Sherif, *Int. J. Electrochem. Sci.*, 7 (2012) 1482.
58. El-Sayed M. Sherif, R.M. Erasmus, J.D. Comins, *J. Appl. Electrochem*., 39 (2009) 83.
59. El-Sayed M. Sherif, *J. Appl. Surf. Sci*., 252 (2006) 8615.
60. El-Sayed M. Sherif, Corrosion Inhibition in Chloride Solutions of Iron by 3-Amino-1,2,4-triazole-5-thiol and 1,1'-Thiocarbonyldiimidazole, *Int. J. Electrochem. Sci.*, 7 (2012) In Press.
61. H. Ma, S. Chen, L. Niu, S. Zhao, S. Li, D. Li, *J. Appl. Electrochem*., 32 (2002) 65.